inventions

Article

An IoT-Enabled System for Monitoring and Predicting Physicochemical Parameters in Rosé Wine Storage Process

Xu Zhang *, Jihong Yang, Ruijie Zhao, Ziquan Qin and Zhuojun Xie

College of Enology, Northwest A&F University, Xianyang 712100, China
* Correspondence: zhang_xu@nwafu.edu.cn

Abstract

The evolution of the winemaking industry towards intelligent and digitalized systems is crucial for precision winemaking and ensuring product safety. In this context, the Internet of Things (IoT) provides a key strategy for real-time monitoring and data management throughout the winemaking process. However, comprehensive multi-parameter IoT-based monitoring and time-series prediction of physicochemical parameters during storage are currently lacking, limiting the ability to assess storage conditions and provide early warning of quality deterioration. To address these gaps, a multi-parameter IoT monitoring system was designed and developed to track conductivity, dissolved oxygen, and temperature in real time. Data were transmitted via a 4th-generation (4G) mobile communication module to the TLINK cloud platform for storage and visualization. An 80-day storage experiment confirmed the system's reliability for long-term monitoring, and analysis of parameter trends demonstrated its effectiveness in assessing storage conditions and wine quality evolution. Furthermore, Long Short-Term Memory (LSTM), Gated Recurrent Unit (GRU), Temporal Convolutional Network (TCN) models, and Autoregressive Integrated Moving Average (ARIMA) were implemented to predict physicochemical parameter trends. The TCN model achieved the highest predictive performance, with coefficients of determination (R^2) of 0.955, 0.968, and 0.971 for conductivity, dissolved oxygen, and temperature, respectively, while LSTM and GRU showed comparable results. These results demonstrate that integrating IoT-based multi-parameter monitoring with deep learning time-series prediction enables real-time detection of abnormal storage and quality deterioration, providing a novel and practical framework for early warning throughout the wine storage process.

Keywords: wine storage; physicochemical parameters; deep learning; IoT; time series prediction

check for updates

Academic Editor: Ismail Fidan

Received: 15 August 2025
Revised: 18 September 2025
Accepted: 21 September 2025
Published: 24 September 2025

Citation: Zhang, X.; Yang, J.; Zhao, R.; Qin, Z.; Xie, Z. An IoT-Enabled System for Monitoring and Predicting Physicochemical Parameters in Rosé Wine Storage Process. *Inventions* **2025**, *10*, 84. https://doi.org/10.3390/inventions10050084

1. Introduction

Rosé wine has gained increasing popularity among younger consumers in recent years [1] due to its pink hue, fruity aroma, low alcohol-by-volume, and sessionable profile, resulting in a steady rise in both production and sales [2]. Compared to red and white wines, rosé wine is more vulnerable to external factors such as temperature and oxygen during storage [3]. Dissolved oxygen is a direct participant in the oxidation process of wine. The higher the concentration of dissolved oxygen, the more complete and faster the oxidation reactions proceed, making it a core factor leading to wine spoilage [4,5]. An increase in wine temperature significantly accelerates the rates of various biochemical reactions in the wine, including oxidative reactions that cause spoilage [6], leading to a faster loss of fresh fruit aromas and the development of off-flavors [7]. Changes in electrical conductivity—usually an increase—can serve as an indicator of oxidative deterioration, as it reflects the rising concentration of ions produced by oxidation reactions in the wine [8], suggesting that irreversible chemical spoilage may have already occurred [9]. Therefore, real-time monitoring of these critical parameters during the storage phase is essential for maintaining product quality, extending shelf life, and achieving precise quality control.

Traditional methods for measuring dissolved oxygen, electrical conductivity, and temperature in liquids primarily rely on manual sampling and offline analysis, which are cumbersome and result in significant delays in obtaining data [10]. With the development of Internet of Things (IoT) technologies toward miniaturization and low power consumption, real-time, in situ monitoring of multiple parameters has become increasingly feasible. A wireless monitoring system was developed using Arduino-based technology, with sensor nodes embedded in barrel bungs to measure physical and chemical parameters, including temperature, of wine during barrel aging [11]. In [12], a multipurpose and low-cost sensor was presented for monitoring the temperature of wine in barrels during two of the most important stages of winemaking: fermentation and maturation. Morais et al. [13] developed a distributed monitoring system based on IoT to monitor temperature, dissolved oxygen, and other parameters during Tawny Port wine aging in oak barrels. Online monitoring methods for electrical conductivity in wine have been proposed in a study [14]; however, monitoring methods based on IoT technology have not yet been reported in the literature.

A large volume of historical time-series data on the physicochemical parameters of wine can be continuously monitored through IoT technology, while time-series forecasting models can uncover underlying patterns and reveal potential future trends [15]. In the analysis of wine-related data, time-series forecasting models have been developed to study the trends of economic data, such as sales [16] and prices [17]; however, time-series prediction research focusing on the physicochemical parameters of wine has not yet been reported in the literature. In recent years, deep learning models have demonstrated remarkable capabilities in time-series forecasting tasks due to their strong nonlinear feature extraction and temporal dependency learning abilities. Models such as Long Short-Term Memory (LSTM), Gated Recurrent Unit (GRU), and Temporal Convolutional Networks (TCNs) are particularly effective in capturing long-term trends and complex temporal dynamics [18,19], making them well-suited for forecasting over extended time horizons. The applications of LSTM, GRU, and TCN models to the prediction of water quality parameters have been reported [20,21].

To enable comprehensive monitoring of the wine storage process and provide early warning of potential quality deterioration, this study designed and implemented a real-time, Internet of Things (IoT)-based system for continuous online acquisition of dissolved oxygen, electrical conductivity, and liquid temperature during rosé wine storage. The collected data were transmitted to a cloud platform for visualization and management. Leveraging these time-series physicochemical data, deep learning models were developed to predict parameter trends. Unlike conventional single-parameter or offline monitoring methods, this integrated approach allows continuous, multi-parameter tracking combined with predictive analysis, providing a novel and intelligent framework for wine storage management and serving as a methodological reference for time-series prediction of physicochemical parameters in wine.

The overall framework of the proposed system is illustrated in Figure 1, which depicts the process from sample monitoring to data transmission, cloud management, predictive modeling, and decision support.

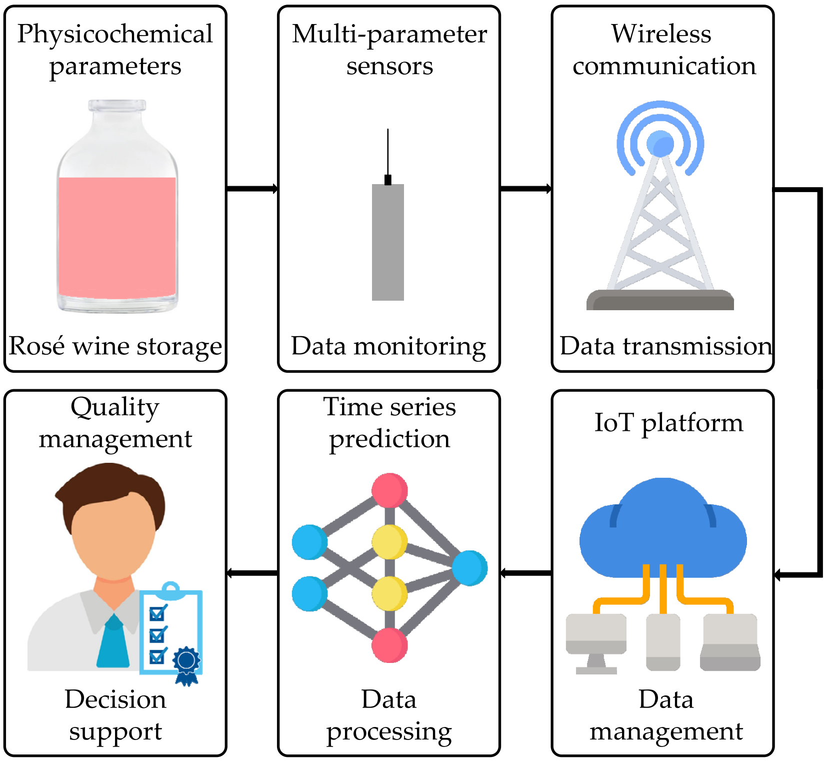

Figure 1. Overall framework of the IoT-based monitoring and prediction system for rosé wine storage.

2. Materials and Methods

2.1. Design of the Monitoring Device for Physicochemical Parameters in Rosé Wine

GD52-RS500A (Gandan, Handan, China): The GD52-RS500A sensor is capable of simultaneously measuring dissolved oxygen, liquid temperature, and electrical conductivity. This sensor features an integrated hardware design in which different signal types share a common communication channel. This approach significantly reduces the overall device size. It supports the standard MODBUS Remote Terminal Unit (MODBUS/RTU) communication protocol with RS-485 digital signal output. The housing is made of 316L stainless steel, a chemically stable material commonly used in fermentation tanks due to its excellent resistance to corrosion caused by acidic substances in wine.

DR154 (USR, Jinan, China): DR154 is a high-speed, low-latency wireless data transfer unit (DTU) based on 4th-generation (4G) mobile communication technology. Its dimensions are extremely compact, approximately the size of a lipstick. It supports a wide input voltage range (5 to 24 volts direct current), making it suitable for diverse application environments. Users can configure parameters such as the gateway mode, serial port settings, and socket server address by scanning a Quick Response code with a smartphone, instead of using a serial cable and computer. With a built-in embedded subscriber identity module (eSIM) card, the device connects to the network immediately upon power-up. The DTU does not perform any processing on the data packets and transmits them directly, operating in a transparent transmission mode.

T60D (MEAN WELL, Guangzhou, China): T60D serves as a power converter that transforms a 220 volts alternating current input into three direct current outputs (5 volts, 12 volts, and 24 volts), with the 12 volts output specifically utilized for powering the 4G DTU and the sensor. It delivers a stable direct current output, with a ripple noise level of 100 mVp-p. It is also designed with overcurrent, overload, and short-circuit protection features, thereby ensuring a high level of electrical safety.

Table 1 lists the models and prices of the modules integrated into the monitoring device, with a total hardware cost of 369.00 United States dollars, which is comparable to the combined cost of separate single-parameter sensors for temperature, dissolved oxygen, and electrical conductivity. Due to the higher level of integration in the GD52-RS500A, the overall device volume is significantly smaller than that of conventional multi-parameter sensors that simply combine independent modules for each parameter.

Table 1. Table of module models and prices.

Module	Model	Size	Price (USD)
Sensor module	GD52-RS500A	246.5 mm × Φ 44 mm	348.00
Data transmission module	DR154 DTU	74 mm × 24 mm×22 mm	14.60
Power module	T60D	159 mm × 97 mm × 38 mm	6.40

The GD52-RS500A multi-parameter sensor measures electrical conductivity based on the two-electrode principle, dissolved oxygen via the ultraviolet fluorescence principle, and temperature using the thermistor principle. The performance specifications of the sensor are listed in Table 2, demonstrating its capability for precise monitoring of the physicochemical parameters of wine. The sensor incorporates a built-in control program for automated data acquisition, periodically collecting raw electrical signals of the parameters at a preset interval of one minute. The acquired signals are processed through amplification circuitry and an analog-to-digital converter to obtain digital signals, which are subsequently processed by a microcontroller. These are then transmitted via an RS-485 interface to a 4G DTU wireless transmission terminal. The DTU receives the RS-485 signals from the GD52-RS500A sensor and establishes bidirectional communication with the TLINK IoT platform under a transparent transmission mode. Through hardware integration and program control, the system achieves a fully automated workflow from parameter sensing to wireless transmission and cloud-based visualization. Figure 2 illustrates the scheme of the monitoring device hardware structure and IoT system architecture.

Table 2. Table of the sensor technical specifications.

Parameters	Detection Range	Resolution	Accuracy	Detection Principle
Conductivity	1.0~2000 µS/cm	1 µS/cm	±2.5%FS	Two-electrode
Dissolved oxygen	0~20 mg/L	0.01 mg/L	± 0.4	Ultraviolet fluorescence
Temperature	0~40 °C	0.1 °C	±0.3 °C	Thermistor

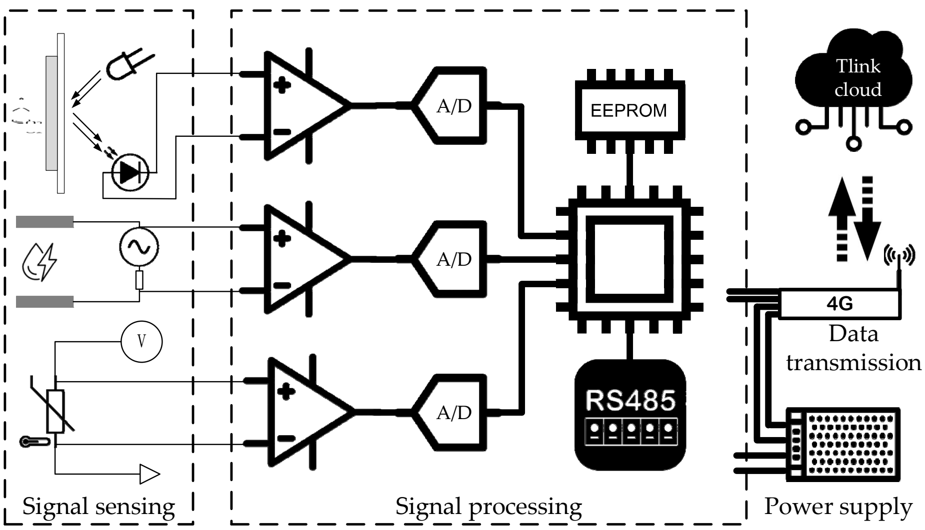

Figure 2. Scheme of the monitoring device hardware structure and IoT system architecture.

2.2. IoT Cloud Configuration Design

TLINK is an IoT platform that supports the development of cloud-based configurations for a variety of application scenarios. Users log in to TLINK to create and manage virtual devices and establish connections with monitoring devices via the MODBUS/RTU protocol. The platform decodes data packets and visualizes real-time monitoring data. In this study, scrolling tables and composite curves were inserted and linked to the devices for the real-time display of three physicochemical parameters during the storage process. Subsequently, relevant components were added and bound to the devices to present information such as online status, connection status, and alarm status. Additional elements, including images, time, air quality, weather, and geographic location, were also incorporated to enhance the functionality of the monitoring interface.

2.3. Monitoring Test of Physicochemical Parameters During Rosé Wine Storage

The monitoring period of this experiment spanned from 22 April to 11 July 2025, lasting a total of 80 days. The monitoring device was placed in the underground wine cellar of the College of Enology, Northwest A&F University. Prior to the experiment, the sensor was rinsed with deionized water and disinfected with alcohol, and then immersed in a glass fermentation tank containing rosé wine, ensuring that the probes for dissolved oxygen, electrical conductivity, and temperature were fully submerged in the wine. The fermentation tank was subsequently sealed, and the entire device was shielded from light. The prepared device was positioned on a flat surface within the cellar, connected to the TLINK cloud platform, and configured to transmit real-time monitoring data. As shown in Figure 3, the monitoring test of physicochemical parameters during rosé wine storage is presented.

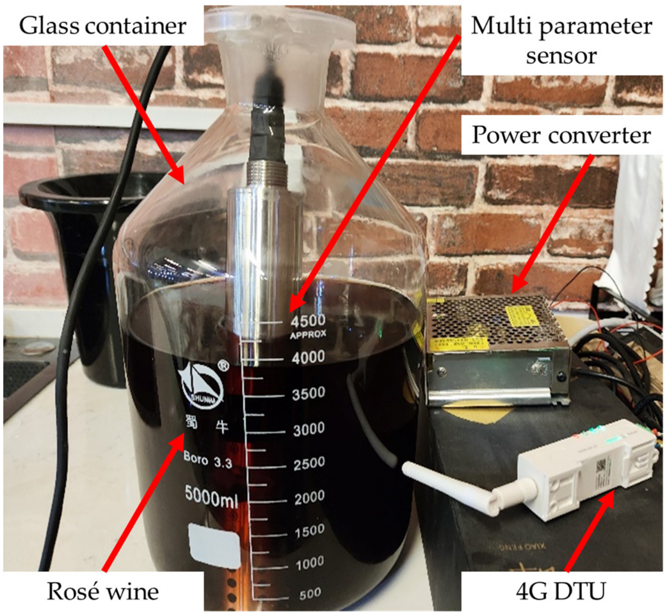

Figure 3. Monitoring test of physicochemical parameters during rosé wine storage.

2.4. Time-Series Prediction Models

2.4.1. Data Preprocessing

The raw water quality monitoring data (dissolved oxygen, electrical conductivity, and temperature) were stored in Excel format, containing timestamps and corresponding measurement values. First, the "time" field was converted to the *datetime* type and sorted in chronological order. To eliminate the impact of irregular sampling intervals on model training, the data were resampled on an hourly basis using the *pandas.resample('H')* method to compute the hourly mean values, and rows with missing data were removed (*dropna()*).

To improve training stability, all the parameters were normalized to the range $[-1, 1]$ using the *MinMaxScaler*. A sliding time window of length t was then constructed, in which the observations from the previous t time steps served as input features, and the observation at the $(t + 1)$-th time step served as the prediction target.

The dataset was split into training and testing sets in a 3:1 ratio according to chronological order, ensuring that all testing data occurred strictly after the training data to prevent information leakage.

2.4.2. Model Construction

In this study, the physicochemical data of rosé wine were used as input for three deep learning architectures—LSTM, GRU, and TCN—to learn patterns from historical variations and predict future trends.

LSTM, a specialized type of recurrent neural network (RNN), retains and updates long-term dependencies through input, forget, and output gates. The proposed LSTM model comprised two hidden LSTM layers with 64 and 32 neurons, respectively, using the *tanh* activation function. A dropout rate of 0.2 was applied between layers to mitigate overfitting, and the final output was produced via a fully connected layer.

The GRU architecture, which simplifies the LSTM design by utilizing only update and reset gates, achieves higher computational efficiency while maintaining comparable performance. The GRU model in this study adopted a similar configuration to the LSTM model, consisting of two hidden layers with 64 and 32 neurons, respectively, a dropout rate of 0.2, and a fully connected output layer.

The TCN architecture leverages causal and dilated convolutions for long sequence modeling, offering parallel computation advantages and avoiding gradient vanishing issues inherent in recurrent structures. The TCN model was constructed using multiple one-dimensional convolutional layers with a kernel size of 3, dilation factors of 1, 2, 4, and 8, and 64 channels. The ReLU activation function was applied, and residual connections were incorporated after each convolutional layer to enhance stability. Table 3 presents the key hyperparameters of the LSTM, GRU, and TCN models, highlighting their input features, architecture settings, and training configurations.

Table 3. Key hyperparameters of the LSTM, GRU, and TCN models.

Parameter	LSTM	GRU	TCN
Input features	3	3	3
Time steps	24	24	24
Hidden units	64	64	64
Number of layers	2	2	3
Kernel size	-	-	3
Number of channels	-	-	[64, 64, 64]
Batch size	32	32	32
Learning rate	0.001	0.001	0.001
Optimizer	Adam	Adam	Adam
Loss function	MSE	MSE	MSE
Epochs	100	100	100
Early stopping patience	12	12	12

As a comparison to the deep learning models, an ARIMA (AutoRegressive Integrated Moving Average) model was constructed for each rosé wine parameter. The ARIMA model, defined by its order (p, d, q), was fitted to the training data using maximum likelihood estimation, and forecasts were generated for the testing set. Unlike LSTM, GRU, and

TCN, which are data-driven neural networks capable of capturing complex nonlinear dependencies, ARIMA is a classical statistical model that explicitly models linear temporal correlations and trends in stationary or differenced time-series.

2.4.3. Model Training and Evaluation Indicators

The models were trained using the Adam optimizer, with the mean squared error (MSE) as the loss function, a batch size of 32, and a maximum of 100 training epochs. An Early Stopping strategy was employed, whereby training was terminated if the training loss failed to decrease for 12 consecutive epochs, and the model parameters were reverted to the best-performing weights to prevent overfitting.

The coefficient of determination for both the training set (R^2_{train}) and the test set (R^2_{test}), along with the root mean square error for training ($RMSE_{train}$) and test ($RMSE_{test}$), were calculated to evaluate the performance of models. All the data preprocessing, model construction, and training procedures were programmed in PyCharm Community Edition 2024.2.1 (JetBrains, Prague, Czech Republic).

3. Results

3.1. IoT Cloud Configuration

Figure 4 shows the interface layout of the physicochemical parameter monitoring system's cloud configuration. Device and connection status information are displayed in the upper-left corner, while the right section provides weather conditions and equipment geographical locations. A scrolling table in the lower-left corner presents the monitoring data for the past four minutes, and the data trend curves are shown in the lower center. Due to the significant differences in magnitude among the three parameters and their relatively slow variation, the curves appear approximately linear. The IoT platform can store, query, and download historical monitoring data for up to three months, facilitating long-term trend analysis and traceability. Users can configure triggers for threshold and disconnection alerts; when a parameter exceeds the set threshold or a device loses connection, notifications are promptly sent to administrators via text message or linked WeChat accounts. This functionality enables wineries to quickly detect anomalies during storage and efficiently manage and maintain monitoring devices. The cloud configuration system is built on the open-source TLINK platform, offering wineries a fast and low-cost solution for implementing IoT-based monitoring.

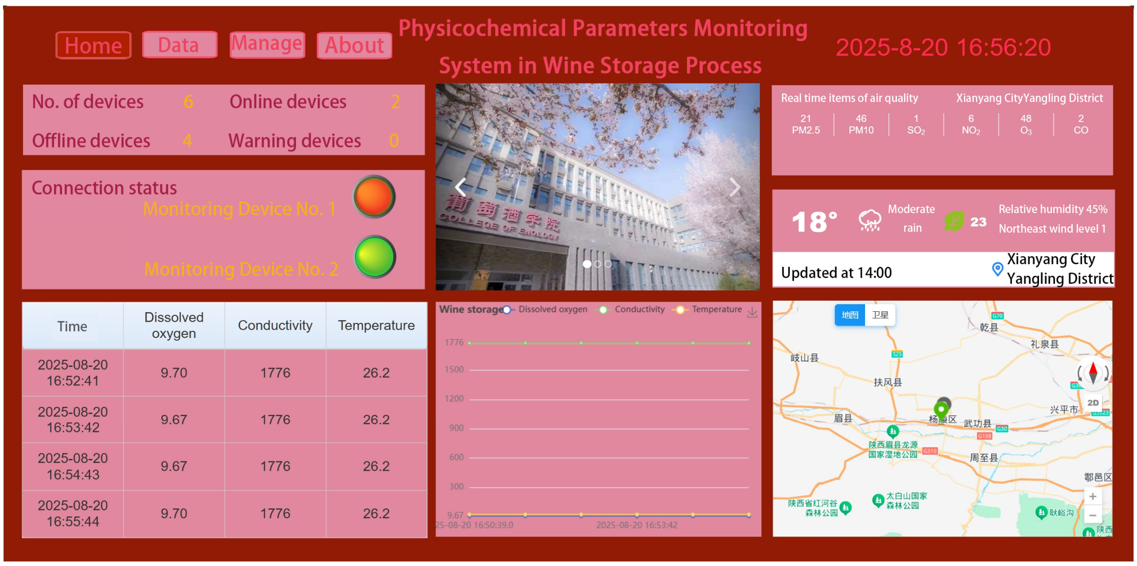

Figure 4. The IoT cloud configuration for the rosé wine storage morning system.

3.2. The Changes in Physicochemical Parameters in Rosé Wine During Storage

Over the 80-day storage period of rosé wine, continuous monitoring was conducted at a 1 min sampling interval, yielding a total of 115,200 data points per parameter. The multi-parameter monitoring device accurately measured the three physicochemical parameters and maintained stable wireless connectivity and power supply in the underground wine cellar, demonstrating its reliability for long-term monitoring. For ease of subsequent data processing and analysis, the parameters were averaged hourly. Figure 5 shows the variation curves of dissolved oxygen, electrical conductivity, and temperature during storage. The three parameters exhibited similar overall trends, and the entire storage process was divided into four stages (S1–S4) based on their variation characteristics, as indicated by the dashed lines in the figure.

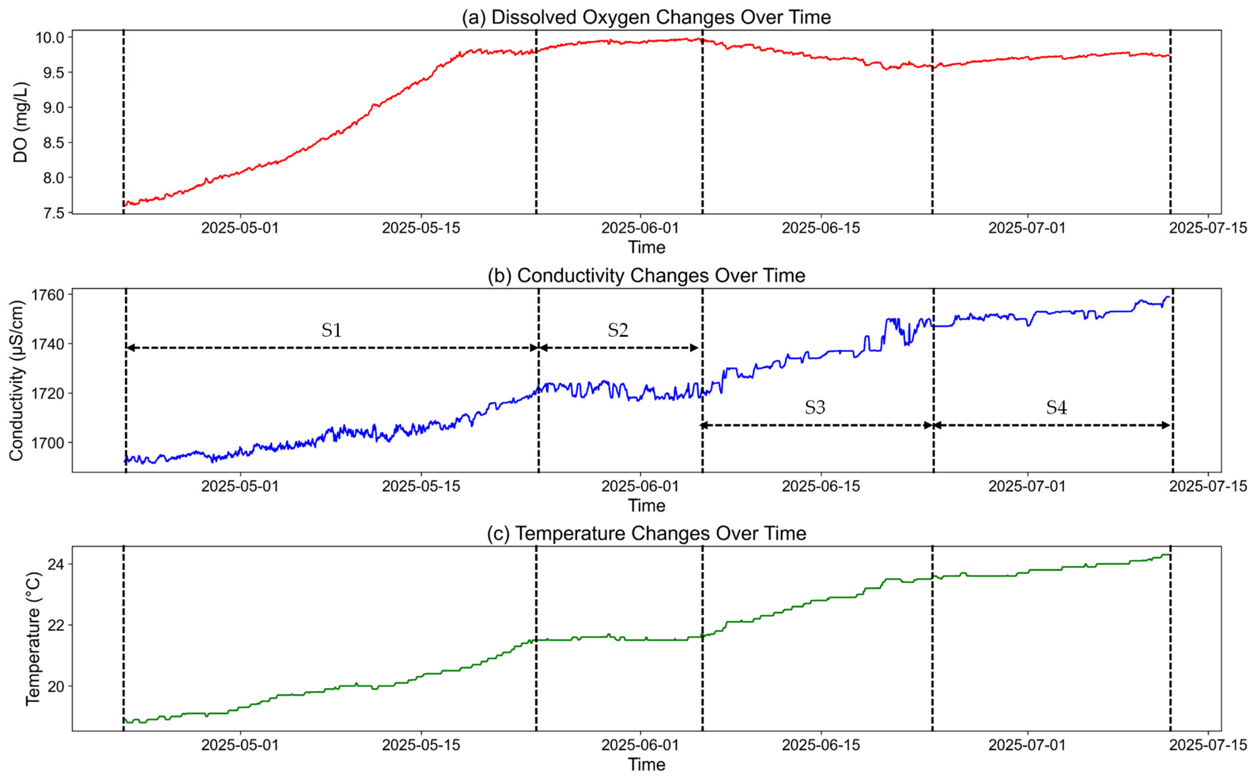

Figure 5. The physicochemical parameters obtained by the rosé wine storage monitoring device, averaged at one-hour intervals: (**a**) trend of dissolved oxygen over time; (**b**) trend of temperature over time; (**c**) trend of conductivity over time.

In stage S1 (from 22 April to 24 May), all three parameters showed a gradual increase. Dissolved oxygen rose from 7.58 mg/L to 9.80 mg/L, reaching a stable state earlier than the other two parameters. Electrical conductivity increased from an initial value of 1689 μS/cm to 1720 μS/cm, while temperature slowly increased from 18.9 °C to 21.5 °C. In stage S2 (from 24 May to 6 June), the three parameters remained relatively stable. Temperature showed little variation and remained around 21.5 °C, dissolved oxygen reached a saturated and steady state at approximately 9.95 mg/L, while electrical conductivity fluctuated within the range of 1718–1730 μS/cm. In stage S3 (from 10 June to 24 June), the three parameters exhibited noticeable changes. Temperature increased from 21.6 °C to 23.6 °C due to the influence of ambient conditions, electrical conductivity rose from 1718 to 1753 μS/cm, and dissolved oxygen showed a decreasing trend, declining from 10.00 mg/L to 9.55 mg/L. In stage S4 (from 24 June to 11 July), the three parameters increased gradually. Temperature rose from 23.5 °C to 24.3 °C, electrical conductivity increased from 1747 to 1759 μS/cm, and dissolved oxygen slightly increased from 9.56 mg/L to 9.80 mg/L.

3.3. The Time-Series Prediction Results of Physicochemical Parameters in Rosé Wine Based on Deep Learning Models

Table 4 presents the prediction results of physicochemical parameters of rosé wine using the LSTM, GRU, TCN, and ARIMA models based on hourly averaged data. The LSTM model achieved test set coefficients of determination of 0.956 and 0.960 for dissolved oxygen and temperature, respectively, which were higher than that for electrical conductivity (R^2 = 0.946). The GRU model yielded slightly better predictive performance than the LSTM model, while the TCN model further improved prediction accuracy, with all R^2 values exceeding 0.950. In contrast, ARIMA, used as a baseline model, showed lower overall performance than the deep learning models, with its highest R^2 being 0.946.

Table 4. Prediction results of physicochemical parameters of rosé wine using LSTM, GRU, TCN, and ARIMA models based on hourly averaged data.

Model	**Parameter**	$\mathbf{R}^2_{train}$	$\mathbf{RMSE}_{train}$	$\mathbf{R}^2_{test}$	$\mathbf{RMSE}_{test}$
LSTM	Conductivity	0.973	2.489	0.946	0.718
	Dissolved oxygen	0.983	0.102	0.956	0.012
	Temperature	0.985	0.167	0.960	0.045
GRU	Conductivity	0.974	2.413	0.947	0.712
	Dissolved oxygen	0.984	0.100	0.957	0.012
	Temperature	0.985	0.167	0.961	0.045
TCN	Conductivity	0.977	2.297	0.951	0.695
	Dissolved oxygen	0.988	0.085	0.964	0.011
	Temperature	0.990	0.134	0.966	0.042
ARIMA	Conductivity	0.958	3.109	0.930	0.830
	Dissolved oxygen	0.971	0.133	0.944	0.014
	Temperature	0.975	0.207	0.946	0.052

Figure A1 in Appendix A shows the time-dependent variation curves of the physicochemical parameters based on 3 h averaged data, and Table 5 summarizes the corresponding prediction results. Compared with Table 4, all the models achieved improved accuracy. This improvement can be attributed to the 3 h averaging, which reduced short-term fluctuations and yielded smoother trends in the data. Among the models, the TCN model achieved the best overall performance, the GRU model outperformed the LSTM model slightly, while the ARIMA model remained the least accurate. In terms of parameter-specific performance, dissolved oxygen achieved higher R^2 values than electrical conductivity, but slightly lower values than temperature.

Table 5. Prediction results of physicochemical parameters of rosé wine using LSTM, GRU, TCN, and ARIMA models based on three-hour averaged data.

Model	**Parameter**	$\mathbf{R}^2_{train}$	$\mathbf{RMSE}_{train}$	$\mathbf{R}^2_{test}$	$\mathbf{RMSE}_{test}$
LSTM	Conductivity	0.978	2.251	0.950	0.724
	Dissolved oxygen	0.987	0.089	0.962	0.011
	Temperature	0.989	0.136	0.965	0.042
GRU	Conductivity	0.979	2.184	0.951	0.724
	Dissolved oxygen	0.989	0.082	0.963	0.011
	Temperature	0.990	0.136	0.965	0.042
TCN	Conductivity	0.984	1.912	0.955	0.705
	Dissolved oxygen	0.994	0.060	0.968	0.011
	Temperature	0.996	0.080	0.971	0.039
ARIMA	Conductivity	0.965	2.819	0.936	0.778
	Dissolved oxygen	0.977	0.116	0.948	0.013
	Temperature	0.979	0.192	0.951	0.050

4. Discussion

The present study designed and developed an IoT system for monitoring the storage parameters of rosé wine. During an 80-day monitoring experiment, the system was able to record changes in conductivity, dissolved oxygen, and temperature in real time, and transmit the data to the TLINK cloud platform for storage and visualization. Compared with previously reported devices that combine single-parameter sensors [22,23], the present system features higher integration and a more compact form factor, enabling deployment in various wine storage containers such as stainless steel tanks, glass fermentation vessels, and oak barrels. The experimental results demonstrate that the developed monitoring device can be used for long-term monitoring of wine storage, effectively reflecting changes in the storage environment while also indirectly capturing the dynamic evolution of wine quality.

The variation trends of the three parameters can generally be divided into a gradual increase phase and a slow increase phase. Temperature changes were strongly influenced by seasonal warming—in Yangling District, Xianyang City, the daily temperature range increased from 9–21 °C on 22 April to 24–36 °C by 11 July. The increase in temperature accelerated the thermal motion of molecules in the wine and enhanced the dissolution and diffusion of gas molecules in the headspace, resulting in a gradual rise in dissolved oxygen content during the early stage, which subsequently stabilized in the later stage. The dissolved oxygen levels observed in this study were notably higher than those reported in [24,25] and comparable to those of wine stored in a glass cup in [26], indicating inadequate sealing performance of the glass container used in this experiment. Elevated temperatures accelerated redox reactions in the wine, thereby increasing its electrical conductivity [27] and resulting in a change trend that showed a certain degree of synchrony with temperature. During rosé wine storage, a continuous increase in dissolved oxygen may accelerate oxidation reactions of phenolic compounds and pigments, causing progressive browning, while higher temperatures may promote the degradation of aroma compounds and the transformation of flavor substances, diminishing the freshness and fruity character of the wine [28]. These observations are consistent with the sensory evaluation of color and aroma at the end of the experiment. Therefore, maintaining proper sealing during storage is crucial for preserving wine quality [29].

The comparison of the prediction results among the three deep learning models shows that the performance of LSTM and GRU is quite similar, which may be related to their model architectures. Both belong to gated recurrent neural networks (Gated RNNs), with GRU being a variant of LSTM featuring a simplified structure that only includes an update gate and a reset gate, resulting in fewer parameters [30]. In contrast, the TCN model demonstrates superior predictive performance, likely due to its advantages in multi-scale feature extraction and long-term dependency modeling [31]. Study [32,33] also employed the same three models to predict water quality parameters, and the results were consistent with those of the present study. Due to their advantages in capturing complex nonlinear relationships and long-term dependencies in time-series, the LSTM, GRU, and TCN models achieved better predictive performance for the physicochemical parameters of rosé wine than the ARIMA model.

The comparison of the prediction results for the three parameters indicates that all the models achieved good fitting performance for temperature, with slightly better results than for dissolved oxygen, while the lowest performance was observed for electrical conductivity. This discrepancy may be attributed to the characteristics of the parameter variation curves. As shown in Figure 5, after resampling the original per-minute measurements into hourly averages, the temperature curve appears the smoothest, whereas the conductivity curve exhibits the most pronounced fluctuations. In contrast, Figure A1 demonstrates that resampling into 3 h averages further reduced local fluctuations, resulting in smoother variation curves for all physicochemical parameters.

The physicochemical parameter monitoring device can be directly installed in stainless steel storage tanks or fixed on the inner wall of oak barrels. By logging into the IoT system via computers or mobile devices, users can monitor in real time the physicochemical changes in wine during storage and aging and receive abnormal alarm notifications. Previous research [11] mainly focused on monitoring a limited set of parameters, such as temperature or pH, with measurements constrained in scope and analysis restricted to the data acquisition level. In contrast, the present study expands the monitoring framework to include multiple physicochemical parameters, such as dissolved oxygen and conductivity, which are critical for evaluating wine storage and aging. Furthermore, by integrating deep learning models (LSTM, GRU, and TCN), the system strengthens data processing and predictive analysis capabilities. This multi-parameter monitoring and forecasting approach provides a more comprehensive solution, offering greater practical value for wineries in storage management and quality control. On the one hand, the system enables timely detection of abnormal fluctuations in wine quality and evaluation of the maturation state during aging, thereby maximizing product quality assurance; on the other hand, it provides robust guidance for optimizing storage conditions, such as container sealing and temperature regulation.

The integrated multi-parameter sensors need to be immersed in wine to monitor the relevant parameters, and therefore, the devices must be disinfected during installation to prevent potential microbial contamination. Due to the limitations of the integrated wireless communication module, the monitoring system can only be deployed in cellars or wineries with 4G signal coverage. The device is powered by a switched-mode power supply and will not operate during AC power outages, and its installation locations are further constrained by the AC wiring layout. These factors somewhat limit the deployment flexibility and general applicability of the system and should be carefully considered in practical applications.

5. Conclusions

This study designed and developed a highly integrated IoT system for real-time monitoring of conductivity, dissolved oxygen, and temperature in rosé wine, with the TLINK cloud platform enabling data acquisition, storage, and visualization. The monitoring experiment validated the system's reliability for long-term observation. Analysis of the trends in physicochemical parameters effectively revealed changes in storage conditions, the evolution of wine quality, and the impact of storage conditions on wine quality. These results highlight the necessity of real-time monitoring during wine storage. This integrated system enables continuous, multi-parameter tracking and indirect assessment of wine quality evolution, highlighting its novelty and practical significance.

In this study, LSTM, GRU, TCN, and ARIMA models were established to predict the physicochemical parameters of rosé wine. The results indicate that all four models can accurately predict the trends of these parameters, with the TCN model demonstrating the best predictive performance. Among the three parameters, temperature exhibited the highest fitting accuracy. The findings suggest that integrating IoT-based monitoring with deep learning prediction models can effectively forecast the dynamic changes in physicochemical parameters during wine storage, providing an innovative approach and practical applications for early warning of abnormal storage conditions and quality deterioration.

Author Contributions: Conceptualization, X.Z.; methodology, X.Z.; software, X.Z.; validation, X.Z.; formal analysis, X.Z.; investigation, J.Y., R.Z., Z.Q. and Z.X.; resources, X.Z.; data curation, J.Y., R.Z., Z.Q. and Z.X.; writing—original draft preparation, X.Z.; writing—review and editing, X.Z. and J.Y.; visualization, X.Z.; supervision, X.Z.; project administration, X.Z.; funding acquisition, X.Z. All authors have read and agreed to the published version of the manuscript.

Funding: This research was supported in part by Northwest A&F University under Grant 245202215, and in part by Shanghai Guolan Agricultural Products Co., Ltd. (Shanghai, China) under Grant TG20250495 and Grant TG20250368.

Institutional Review Board Statement: Not applicable.

Informed Consent Statement: Not applicable.

Data Availability Statement: The datasets generated for this study are available upon request from the corresponding author due to ongoing experimental projects and technical restrictions.

Acknowledgments: We sincerely thank the staff from Shanxi Geruite chateau Co., Ltd. (Yuncheng, China) and Shanxi Rongzi chateau Co., Ltd. (Linfen, China) for providing us with the test site and grape samples.

Conflicts of Interest: The authors declare no conflicts of interest. The funding sponsors had no role in the design of the study; in the collection, analyses, or interpretation of data; in the writing of the manuscript; or in the decision to publish the results.

Abbreviations

The following abbreviations are used in this manuscript:

IoT	Internet of Things
LSTM	Long Short-Term Memory
GRU	Gated Recurrent Unit
TCN	Temporal Convolutional Networks
RNN	Recurrent Neural Network
DTU	Data Transfer Unit
MSE	Mean Squared Error
R^2_{train}	Coefficient of Determination for the Training Set
R^2_{test}	Coefficient of Determination for the Test Set
$RMSE_{train}$	Root Mean Square Error for Training Set
$RMSE_{test}$	Root Mean Square Error for Test Set
eSIM	Embedded Subscriber Identity Module
4G	4th-generation
ARIMA	AutoRegressive Integrated Moving Average

Appendix A

Figure A1 shows the physicochemical parameters obtained by the rosé wine storage monitoring device, which were averaged at three-hour intervals.

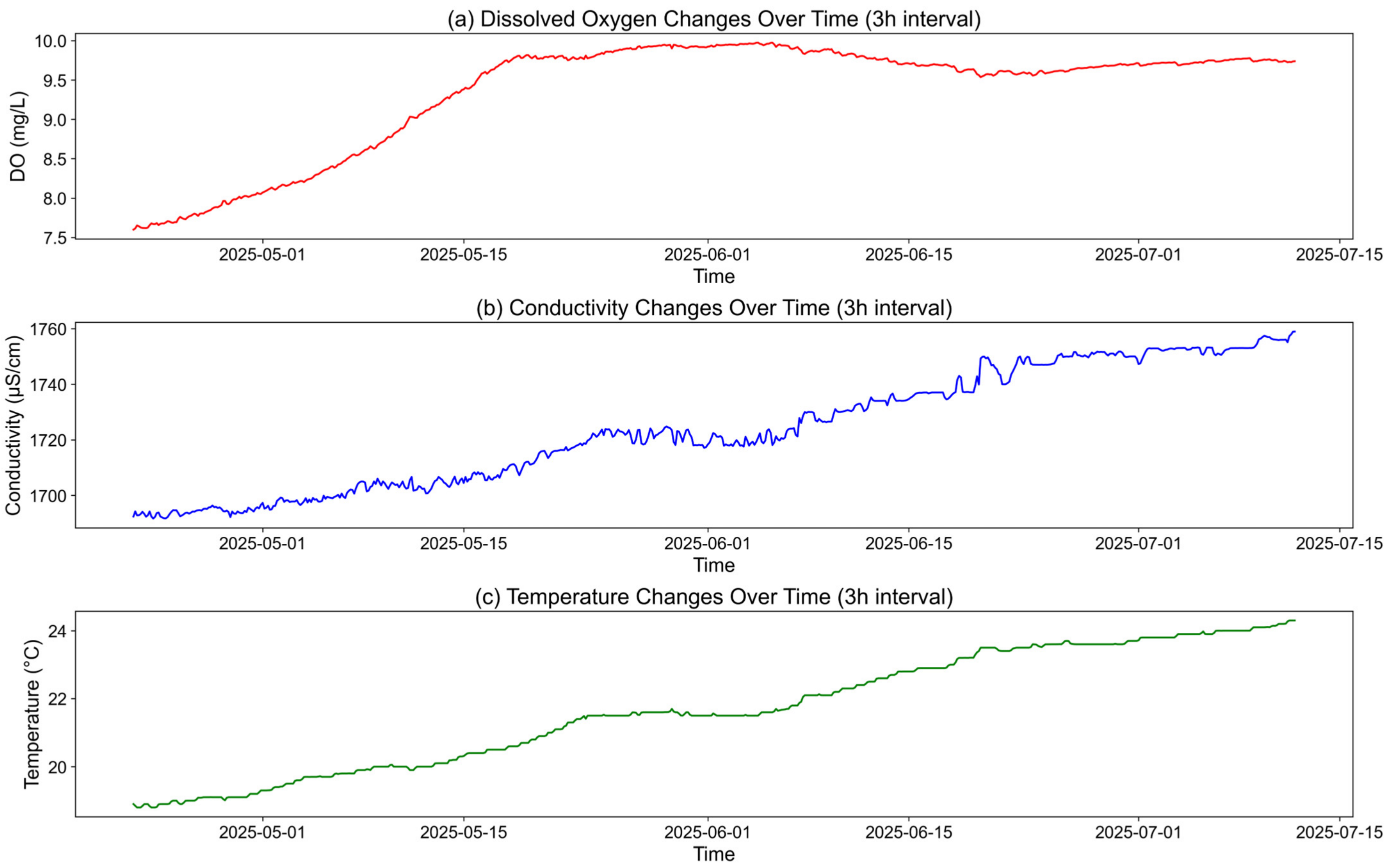

Figure A1. The physicochemical parameters obtained by the rosé wine storage monitoring device, averaged at three-hour intervals: (**a**) trend of dissolved oxygen over time; (**b**) trend of temperature over time; (**c**) trend of conductivity over time.

References

1. Iazzi, A.; Scorrano, P.; Rosato, P.; Grandhi, B. Millennial generation preferences for rosé wine. *Br. Food J.* **2019**, *122*, 2443–2461. [CrossRef]
2. Peres, S.; Giraud-Heraud, E.; Masure, A.; Tempere, S. Rose Wine Market: Anything but Colour? *Foods* **2020**, *9*, 1850. [CrossRef] [PubMed]
3. Medina-Plaza, C.; Dubois, A.; Tomasino, E.; Oberholster, A. Effect of storing conditions (lighting, temperature and bottle color) on rosé wine attributes. *Food Chem.* **2024**, *439*, 138032. [CrossRef] [PubMed]
4. Benucci, I.; Cerreti, M.; Esti, M. Dosing oxygen from the early stages of white winemaking: Effect on oxidation–reduction potential, browning stability, volatile composition, and sensory properties. *Food Chem.* **2024**, *432*, 137243. [CrossRef]
5. Dai, L.; Sun, Y.; Liu, M.; Cui, X.; Wang, J.; Li, J.; Han, G. Influence of Oxygen Management during the Post-Fermentation Stage on Acetaldehyde, Color, and Phenolics of Vitis vinifera L. Cv. Cabernet Sauvignon Wine. *Molecules* **2022**, *27*, 6692. [CrossRef]
6. Deshaies, S.; Cazals, G.; Enjalbal, C.; Constantin, T.; Garcia, F.; Mouls, L.; Saucier, C. Red Wine Oxidation: Accelerated Ageing Tests, Possible Reaction Mechanisms and Application to Syrah Red Wines. *Antioxidants* **2020**, *9*, 663. [CrossRef]
7. Bai, X.; Chen, X.; Li, X.; Tan, F.; Sam, F.E.; Tao, Y. Wine polyphenol oxidation mechanism and the effects on wine quality: A review. *Compr. Rev. Food. Sci. Food Saf.* **2024**, *23*, e70035. [CrossRef]
8. Newair, E.F.; Al-Anazi, A.; Garcia, F. Oxidation of Wine Polyphenols by Electrochemical Means in the Presence of Glutathione. *Antioxidants* **2023**, *12*, 1891. [CrossRef]
9. Chen, X.; Ma, Y.; Diao, T.; Leng, Y.; Lai, X.; Wei, X. Pulsed electric field technology for the manufacturing processes of wine: A review. *J. Food Process Preserv.* **2022**, *46*, e16750. [CrossRef]
10. Amrita, C.M.; Babiyola, D. Analysing the water quality parameters from traditional to modern methods in aquaculture. *Int. J. Sci. Environ. Technol.* **2018**, *7*, 1954–1961.
11. Di Gennaro, S.F.; Matese, A.; Mancin, M.; Primicerio, J.; Palliotti, A. An Open-Source and Low-Cost Monitoring System for Precision Enology. *Sensors* **2014**, *14*, 23388–23397. [CrossRef]
12. Zhang, W.; Skouroumounis, G.; Monro, T.; Taylor, D. Distributed Wireless Monitoring System for Ullage and Temperature in Wine Barrels. *Sensors* **2015**, *15*, 19495–19506. [CrossRef] [PubMed]

13. Morais, R.; Peres, E.; Boaventura-Cunha, J.; Mendes, J.; Cosme, F.; Nunes, F.M. Distributed monitoring system for precision enology of the Tawny Port wine aging process. *Comput. Electron. Agric.* **2018**, *145*, 92–104. [CrossRef]
14. Zhang, Q.; Shen, Y.; Fan, X.; Yan, Y.; García Martín, J.F. Online monitoring of electrical conductivity of wine induced by ultrasound. *CYTA J. Food* **2016**, *14*, 496–501. [CrossRef]
15. Liu, Z.; Zhu, Z.; Gao, J.; Xu, C. Forecast Methods for Time Series Data: A Survey. *IEEE Access* **2021**, *9*, 91896–91912. [CrossRef]
16. Su, Y.; Wang, M.C.; Liu, S. Automated Machine Learning Algorithm Using Recurrent Neural Network to Perform Long-Term Time Series Forecasting. *CMC-Comput. Mat. Contin.* **2024**, *78*, 3529–3549. [CrossRef]
17. Algieri, B.; Iania, L.; Leccadito, A.; Meloni, G. Message in a bottle: Forecasting wine prices. *J. Wine Econ.* **2024**, *19*, 64–91. [CrossRef]
18. Li, W.; Law, K.L.E. Deep Learning Models for Time Series Forecasting: A Review. *IEEE Access* **2024**, *12*, 92306–92327. [CrossRef]
19. Ahmed, D.M.; Hassan, M.M.; Mstafa, R.J. A review on deep sequential models for forecasting time series data. *Appl. Comput. Intell. Soft Comput.* **2022**, *2022*, 6596397. [CrossRef]
20. Li, W.; Zhao, Y.; Zhu, Y.; Dong, Z.; Wang, F.; Huang, F. Research progress in water quality prediction based on deep learning technology: A review. *Environ. Sci. Pollut. Res.* **2024**, *31*, 26415–26431. [CrossRef]
21. Wang, X.; Li, Y. Prediction of mine water quality by the Seq2Seq model based on attention mechanism. *Heliyon* **2024**, *10*, e37916. [CrossRef] [PubMed]
22. Udayakumar, K.; Subiramaniyam, N.P. Deep learning-based production assists water quality warning system for reverse osmosis plants. *H2Open J.* **2020**, *3*, 538–553. [CrossRef]
23. Jan, F.; Min-Allah, N.; Düştegör, D. IoT Based Smart Water Quality Monitoring: Recent Techniques, Trends and Challenges for Domestic Applications. *Water* **2021**, *13*, 1729. [CrossRef]
24. Zhang, T.; Liao, Z.; Li, Z.; Liu, Y.; Liu, Y.; Song, Y.; Qin, Y. Dynamic changes in dissolved oxygen concentration, microbial communities, and volatile compounds during industrial oak-barrel fermentation of Sauvignon Blanc wine. *Food Res. Int.* **2024**, *197*, 115250. [CrossRef]
25. Roussey, C.; Colin, J.; Du Cros, R.T.; Casalinho, J.; Perré, P. In-situ monitoring of wine volume, barrel mass, ullage pressure and dissolved oxygen for a better understanding of wine-barrel-cellar interactions. *J. Food Eng.* **2021**, *291*, 110233. [CrossRef]
26. Giuseppina Paola, P.; Matteo, M.; Arianna, R.; Andrea, V. Effect of Different Glass Shapes and Size on the Time Course of Dissolved Oxygen in Wines during Simulated Tasting. *Beverages* **2018**, *4*, 3. [CrossRef]
27. Yan, Y.; Zhang, Q.; Li, E.; Zhang, Y. Ions in Wine and Their Relation to Electrical Conductivity Under Ultrasound Irradiation. *J. AOAC Int.* **2017**, *100*, 1516–1523. [CrossRef]
28. Oliveira, C.M.; Barros, A.S.; Silva Ferreira, A.C.; Silva, A.M.S. Influence of the temperature and oxygen exposure in red Port wine: A kinetic approach. *Food Res. Int.* **2015**, *75*, 337–347. [CrossRef]
29. Echave, J.; Barral, M.; Fraga-Corral, M.; Prieto, M.A.; Simal-Gandara, J. Bottle Aging and Storage of Wines: A Review. *Molecules* **2021**, *26*, 713. [CrossRef]
30. Shewalkar, A. Performance evaluation of deep neural networks applied to speech recognition: RNN, LSTM and GRU. *J. Artif. Intell. Soft Comput. Res.* **2019**, *9*, 235–245. [CrossRef]
31. Zuo, C.; Wang, J.; Liu, M.; Deng, S.; Wang, Q. An Ensemble Framework for Short-Term Load Forecasting Based on TimesNet and TCN. *Energies* **2023**, *16*, 5330. [CrossRef]
32. Zamani, M.G.; Nikoo, M.R.; Jahanshahi, S.; Barzegar, R.; Meydani, A. Forecasting water quality variable using deep learning and weighted averaging ensemble models. *Environ. Sci. Pollut. Res.* **2023**, *30*, 124316–124340. [CrossRef]
33. Fu, Y.; Hu, Z.; Zhao, Y.; Huang, M. A long-term water quality prediction method based on the temporal convolutional network in smart mariculture. *Water* **2021**, *13*, 2907. [CrossRef]